

Holocene geomagnetic paleointensities: A blind test of absolute paleointensity techniques and materials

Fabio Donadini^{a,*}, Peter Riisager^{b,c}, Kimmo Korhonen^d, Kimmo Kahma^e,
Lauri Pesonen^a, Ian Snowball^b

^a University of Helsinki, Division of Geophysics, Gustaf Hällströmin katu 2, FI-00014 Helsinki, Finland

^b University of Lund, Geobiosphere Science Centre, Department of Geology,
Quaternary Sciences, Sölvegatan 12, S-223 62 Lund, Sweden

^c University of Copenhagen, Geological Museum, Øster Voldgade 5-7, DK-1350 Copenhagen K, Denmark

^d Helsinki University of Technology, Laboratory of Geoenvironmental Technology, Otakaari 1, FI-02015 Espoo, Finland

^e Finnish Institute of Marine Research, Erik Palménin aukio 1, FI-00560 Helsinki, Finland

Received 21 August 2006; received in revised form 11 December 2006; accepted 20 December 2006

Abstract

Through several decades of research, absolute paleointensity estimates have been obtained from a wide range of rocks with varying ages, covering the last 3.45 Ga years. These paleointensity data are crucial to study the past geodynamo and the geological evolution of the Earth's deep interior. However, paleointensity data are often difficult to interpret, and on-going discussions concerning the past geomagnetic field invariably focus on data reliability, and which kind of material, and method, is best suited for absolute paleointensity experiments.

In this paper we blind test paleointensity methods and materials using the new GEOMAGIA50 database that contains all available experimental information about published paleointensity estimates covering the last 50,000 years. Our analysis is built on simple comparisons of results obtained from different materials, and methodologies, to investigate their possible influence on the paleointensity estimate. We also study the effect of various numbers of samples, and dating accuracies. We focus on paleointensity estimates from the last 12,000 years, which includes the Holocene epoch. The advantage of this period is that data have been obtained from a wide array of methodological techniques as well as a wide selection of materials, including both natural ones (e.g. lava flows) and various archaeological artifacts. Our main observations are (i) that well-fired archaeological materials (bricks, potteries, clays, and ceramics) show the best correlation with the rest of the dataset, which we interpret to suggest that these data are the most reliable, and (ii) although paleointensity data obtained from lava flows are slightly more scattered, there is no evidence for paleointensity data from lavas to be significantly lower or higher than other data, irrespective of the methodology.

© 2007 Elsevier B.V. All rights reserved.

Keywords: Paleointensity; Holocene; Database; Paleointensity techniques and materials

1. Introduction

Palaeomagnetism enables us to study planetary magnetic fields in the crucial dimension of time. The paleomagnetic field recorded in Lunar and Martian rocks indicate that they once had operating geodynamos (Collinson, 1993; Weiss et al., 2002), which died out,

* Corresponding author. Tel.: +358 9 191 51008;
fax: +358 9 191 51000.

E-mail address: fabio.donadini@helsinki.fi (F. Donadini).

probably due to significant changes in their deep interiors (Stevenson, 2001). Paleomagnetic studies of the Earth show that its geomagnetic field has existed for at least 3 billion years, but with varying intensity and direction. A more detailed knowledge of the Earth's paleomagnetic field may shed light on the evolution of the geodynamo over different geological time scales. In particular, such knowledge may reveal past variations in heat-flow across the core–mantle–boundary (Glatzmaier et al., 1999) and nucleation and growth of the solid inner core (Tarduno et al., 2006). A detailed knowledge of the Earth's paleomagnetic field is also needed to understand present-day and future changes of our planet. For example, the debates over an imminent reversal (Hulot et al., 2002; Constable and Korte, 2006) and possible links between the Earth's magnetic field and its climate (Gallet et al., 2005) are difficult to settle because our knowledge is limited. One of the key parameters to study these changes is the paleomagnetic field intensity, for short called “paleointensity”, which in virtual axial dipole moment (VADM) terms has today an average value of about $7.9 \times 10^{22} \text{ A m}^2$ (Korte and Constable, 2005). Based on GEOMAGIA, the averaged VADM value using the data from the 20th century corresponds to $8.13 \pm 1.51 \times 10^{22} \text{ A m}^2$. The lowest value ($5.92 \times 10^{22} \text{ A m}^2$) is recorded from Scandinavia (Pesonen et al., 1995), whereas the highest value ($17.26 \times 10^{22} \text{ A m}^2$) stems from Georgia (Burlatskaya et al., 1969). This latter value, however, was obtained from an experiment without alteration checks, hence its reliability might be questionable. Nowadays, the introduction of satellite as well as observatory data makes it possible to get a full geographic coverage of magnetic observation. Recent models based on these observations (e.g. Jackson et al., 2000; Olsen, 2002) show the presence of an intensity minimum close to South America and the South Atlantic (South Atlantic Anomaly).

Unfortunately, it is difficult to find rocks that are ideally suited for absolute paleointensity experiments; they must fulfill a long list of criteria concerning the nature of their magnetization, magnetic mineralogy, magnetic grain size, and magnetic interactions (e.g. Selkin and Tauxe, 2000; Riisager et al., 2002; Valet, 2003). In fact, the vast majority of published absolute paleointensity data stem from geological material that are not ideal, such as volcanic lava flows, dikes, and intrusions. These almost invariably have experienced some alteration, and also contain multi-domain magnetic particles, which are problematic for absolute paleointensity experiments (Riisager and Riisager, 2001). In recent years, focus has turned towards geological materials with a smaller magnetic grain size, e.g. single plagioclase crystals (Tarduno

and Cottrell, 2005) and basaltic glass (Tauxe, 2006). However, the suitability of these geological materials is also debated, and the central question remains: How does one estimate the reliability of paleointensity data and correctly interpret them in terms of actual geomagnetic field variations? Adding to the difficulty of interpreting absolute paleointensity data is the fact that there exist several different experimental techniques and there are many opinions on which methodological approach is best. It is perhaps not surprising, therefore, that discussions concerning the Earth's past geomagnetic field intensity is centered on which kind of material, and which method, is best suited for paleointensity experiments (Heller et al., 2002; Valet, 2003; Smirnov and Tarduno, 2005; Yamamoto and Tsunakawa, 2005), i.e. which paleointensity data to believe and which to discard. To settle these discussions more testing of absolute paleointensity techniques and materials is necessary.

It is difficult to test absolute paleointensity techniques and materials based solely on theoretical models because the magnetization of natural objects is too complex to be fully represented by numerical models. The validity of paleointensity materials and methods is, therefore, best tested experimentally. This is possible, for example, by imparting an artificial thermal remanent magnetization (TRM) in the laboratory, and testing if the paleointensity determination equals the artificial laboratory field intensity (Pan et al., 2002; Hill et al., 2002). The problem with these tests is that it is difficult to fully reproduce the natural environment in the laboratory, which makes it difficult to extrapolate the laboratory observations to rocks and archaeological artefacts. Pesonen et al. (1995) prepared artificial bricks and fired them in the natural Earth's magnetic field in South Finland. In this case, the paleointensity obtained was in good agreement with observatory values for South Finland. Also, it was shown that both classical Thellier and Thellier (1959) and its modified Coe (1967) methodologies give similar results. Interestingly, the bricks were drilled in perpendicular directions to study the fabric anisotropy and some influence on the intensity results was noticed. Another possible approach is to perform paleointensity experiments on young rocks or archaeological artefacts for which the geomagnetic field intensity is known from direct historical observations (e.g. geomagnetic observatory data). In most cases such tests have yielded the correct paleointensity (e.g. Pick and Tauxe, 1993; Cottrell and Tarduno, 1999; Hill and Shaw, 2000; Chauvin et al., 2005; Oishi et al., 2005). However, in other cases, the tests have not been conclusive (Calvo et al., 2002; Yamamoto et al., 2003; Mochizuki et al., 2004; Coe et al., 2004). The different outcomes of these paleointensity tests are difficult to

interpret. One of the main problems interpreting paleointensity data from non-ideal materials is that only part of the blocking/unblocking temperature spectra can be used, and it is often not obvious which part. In such cases, some subjectivity is invariably involved, which is a serious drawback of these experimental paleointensity tests, as researchers may be biased by the fact that they know the correct result at the time they carry out their experiments. To underline the difficulty of experimental tests involving historical paleointensity materials, we note the curious example of a single 1960 Hawaiian lava flow, which produced a correct paleointensity to one group of researchers (Chauvin et al., 2005), but significantly too high paleointensities to another group (Yamamoto et al., 2003) using the exact same experimental technique. Chauvin et al. (2005) suggest that this divergence reflects differences in the way paleointensity data are interpreted. Another serious drawback of the above discussed experimental tests is that they are based on single cooling units. It is perhaps dangerous to draw general conclusions concerning paleointensity techniques and materials based on these small datasets.

In this study we aim to test paleointensity techniques and materials using a different approach. Our analysis is based on the available Holocene paleointensity data, the amount of which has grown significantly in recent years. A particular advantage of Holocene paleointensity data is that they have been obtained from a wide array of methodological techniques, as well as a wide selection of materials, including both natural ones (e.g. lava flows) as well as various archaeological artifacts. Our test is based on comparisons between certain techniques/materials and other techniques/materials of similar age. We believe our analysis has two major advantages: (i) it is based on a very large dataset, and therefore more generally applicable than paleointensity tests involving single cooling units, and (ii) it is blind; meaning that the data stem from periods where the field intensity was not directly known, and there is therefore less reason to suspect researchers to bias their interpretations towards obtaining the “correct answer”. Thus, the data interpretation is possibly less biased than direct tests, where researchers know the correct results.

2. The GEOMAGIA50 absolute paleointensity database and the analysis features

Our analysis is based on the new on-line GEOMAGIA50 database, which in addition to the actual paleointensities, also contains information concerning the materials, paleointensity methods, and other important experimental features. In the following we will

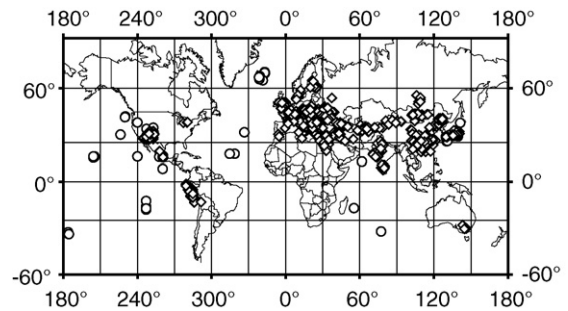


Fig. 1. Distribution of the 3425 Holocene intensity sites of lavas (circles) and archeological artifacts (diamonds) in GEOMAGIA50.

briefly discuss the database information relevant to our analysis, while a more in-depth description of the GEOMAGIA50 database can be found elsewhere (Korhonen et al., in preparation; Donadini et al., 2006; see also “<http://data.geophysics.helsinki.fi/>”). All information in the database was compiled from published papers. In case some details were missing, the author was contacted, and the database was updated wherever possible. Otherwise the information is given as “missing”. Additionally, if no mean value for a study has been reported, this has been calculated by arithmetic mean. The standard deviation then refers to the arithmetic mean and the present GEOMAGIA50 database includes 3425 absolute intensity data for the last 12,000 years; no lake sediment data have been included so far. The geographical and temporal distributions of the data are inhomogeneous. In particular, most determinations originate from moderate latitudes (10–40°N) (Fig. 1) and cover predominantly the last 6000 years (Fig. 2). The geographical distribution of lavas is broad, whereas the distribution of archaeological artefacts centres on Central Europe and Eastern European countries. With the exception of potteries, the coverage of other regions is rather poor.

2.1. Materials

A main motivation for the present study is that the Holocene paleointensity database contains data from many different kinds of material; both natural, e.g. lava flows, as well as several distinct kinds of archaeological objects. The magnetic recording mechanisms are different for many of these materials, and they therefore have different potential error sources. A comparison between the various materials may therefore illustrate various degrees of correlation. Holocene archaeological artefacts that yield paleointensity data of excellent experimental quality (e.g. Casas et al., 2005) are of particular importance. In fact, they form a good basis for testing ambiguous materials. Altogether 13 differ-

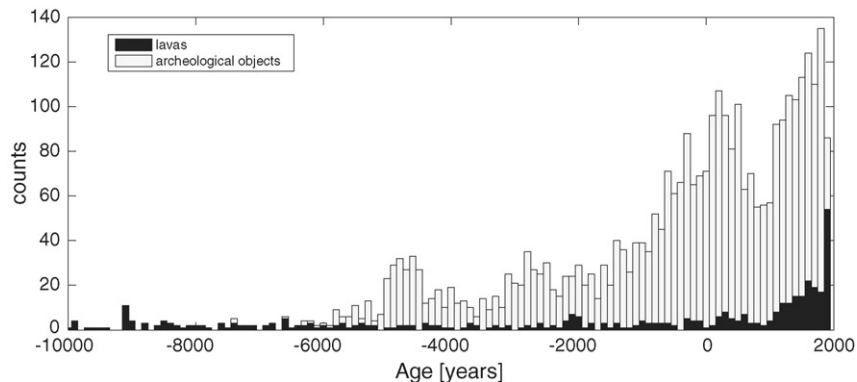


Fig. 2. Distribution of the 3425 Holocene data in time. Data are binned in 100 years intervals, and counts represent the amount of data in each bin.

ent categories of materials exist in the Holocene dataset we analyzed. As shown in Fig. 3a, potteries represent the majority of data (26%), followed by bricks (18%), ceramics (12%), lavas (12%), and baked clays (11%). Six percent of the material used to determine a particular intensity is not described in the original publication, and we mark these data as “not specified” in the database.

2.2. Techniques

We divide absolute paleointensity techniques into four main groups: (i) Thellier with pTRM checks, (ii) Thellier without pTRM checks, (iii) Microwave, and (iv) Shaw techniques. There are several subtypes, so that the GEOMAGIA50 database contains altogether 17 different classifications (Fig. 3b). We will briefly discuss the four main groups of paleointensity experiments below. A more thorough description of paleointensity methods has been given elsewhere (e.g. Selkin and Tauxe, 2000; Valet, 2003).

The Thellier method (Thellier and Thellier, 1959) and its modifications (e.g. Coe, 1967; Yu et al., 2004) are the most widespread and accepted methods for palaeointensity determination. Thellier experiments consist of step-wise thermal demagnetization of NRM and thermal re-magnetization of TRM. Since thermal alteration during laboratory heating can impair the results, the partial thermoremanent magnetisation (pTRM) check (Coe, 1967) is generally employed to detect thermochemical alteration due to laboratory heating. Other types of pTRM checks to monitor the presence of non-ideal magnetic grain sizes have also been introduced (Shcherbakova and Shcherbakov, 2000; Riisager and Riisager, 2001; Krasa et al., 2003). Also, some Thellier paleointensity data have been corrected for fabric and/or shape anisotropy and cooling rate effects (e.g.

Fox and Aitken, 1980). The effect of fabric anisotropy has been studied by determining either the susceptibility, the anhysteretic remanent magnetization (ARM) or the TRM tensor (e.g. Veitch et al., 1984; Genevey and Gallet, 2002; Chauvin et al., 2005), or trying to align the laboratory field and the NRM. In some cases, the anisotropy effect can be averaged out if the sampling is made random. In contrast, the cooling rate effect appears to be systematic for assemblies of SD and PSD grains (e.g. Gómez-Paccard et al., 2006). The shape anisotropy (also called magnetic refraction) appears to be of importance in strongly magnetized structures (e.g. Tarling et al., 1986; Pesonen et al., 1995). However, corrections of anisotropy and cooling rate are not easy to quantify, and are generally not very large and are therefore not considered of major significance for this study. Inspecting Fig. 3b, it turns out that Thellier type paleointensity experiments represent 67% of all data available for the last 12,000 years (Fig. 3a). Roughly half (31%) of the Thellier determinations did not employ any kind of pTRM-checks.

Walton (1991) developed a new technique, which magnetizes and demagnetizes the magnetic carriers using microwaves. In principle, microwaves affect the magnetic carriers in a similar fashion to the normal heating. However, the bulk sample is heated to lower temperatures compared to radiant heating, because the bulk matrix of the sample is left untouched by the microwaves. Hence the possibility of alteration is lower. Also, the experimental procedure requires a shorter time compared to normal Thellier experiments. Despite these two main advantages, a debate arises over whether or not the blocking temperature of the natural cooling material correlates with the unblocking temperature induced by microwaves. Microwave paleointensity data currently represent only 2% of the Holocene dataset. Nevertheless it is an important group because microwave

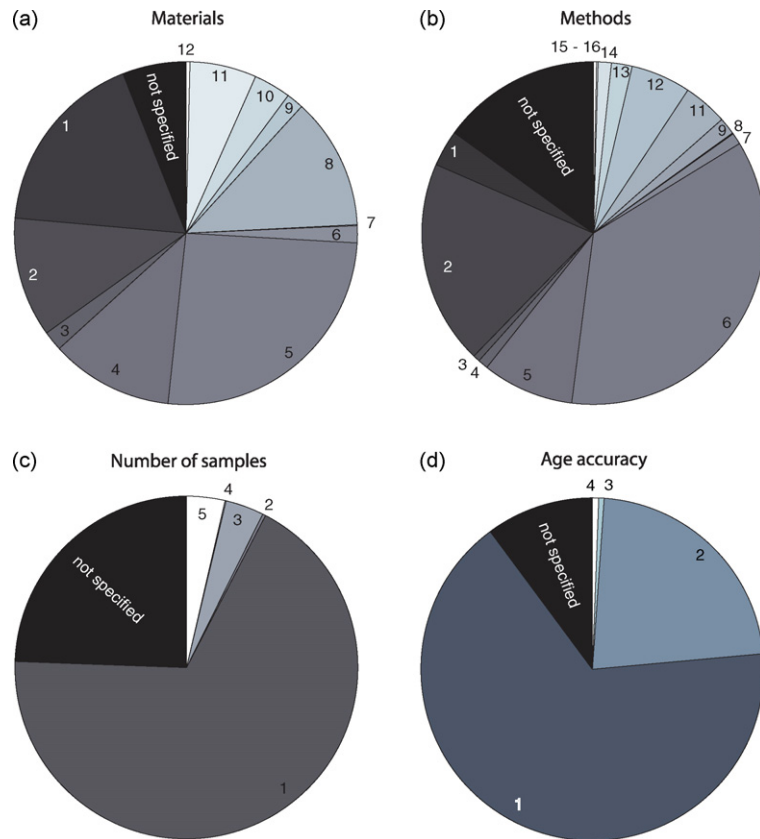


Fig. 3. (a) The distribution of materials during the last 12,000 years: 1 = bricks, 2 = clay, 3 = tiles, 4 = lava, 5 = pottery, 6 = sun-dried objects, 7 = porcelain, 8 = ceramic, 9 = kiln, 10 = oven or hearth, 11 = miscellaneous archaeological objects, 12 = ironslag, 13 = baked rocks. (b) The percentage of methodologies used for determining paleointensities on materials younger than 12,000 years. 1 = Thellier/Coe, pTRM check, anisotropy and cooling rate corrections; 2 = Thellier/Coe, pTRM check, anisotropy or cooling rate correction, 3 = Thellier/Coe, pTRM check, NRM oriented along laboratory field (B_{lab}), cooling rate correction, 4 = Thellier/Coe, pTRM check, NRM oriented along B_{lab} , no cooling rate correction, 5 = Thellier with pTRM checks, no corrections, 6 = Thellier without checks, no corrections, 7 = Shaw, cooling rate correction and anisotropy correction, 8 = Shaw, anisotropy or cooling rate correction, 9 = Shaw, NRM oriented along B_{lab} , cooling rate correction, 10 = Shaw, NRM oriented along B_{lab} , no cooling rate correction, 11 = Shaw, no corrections, 12 = other techniques, 13 = microwave, pTRM checks, 14 = microwave, no pTRM checks, 15 = Thellier/Coe, alteration correction, no cooling and no anisotropy correction, 16 = Thellier without checks, NRM parallel to B_{lab} . (c) Distribution of the amount of samples per intensity determination: 1 = only one sample measured, 2 = two samples and standard deviation higher than 10%, 3 = two samples and standard deviation lower than 10%, 4 = at least three samples with standard deviation higher than 10%, 5 = at least three samples with standard deviation lower than 10%. (d) Age dating error distribution related to the intensity determinations: 1 = accuracy between ± 100 years, 2 = accuracy between ± 500 years, 3 = accuracy between ± 1000 years, 4 = accuracy worse than 1000 years.

paleointensities are considered particularly useful for studies on older geologic samples from the Earth (Halls et al., 2004) and other planetary bodies (Shaw et al., 2001).

Another main part of the Holocene dataset is based on the paleointensity technique introduced by Shaw (1974). He suggested a method consisting of only one TRM acquisition, and instead relying on alternating field demagnetizations, and ARMs to possibly discard parts of the blocking/unblocking temperature spectra that have been influenced by secondary magnetizations or alterations. The main advantage of this technique is the rapidity of its execution. However, debates arise whether

the comparison of ARMs for correction of alteration is an analogy of the TRM. Like Thellier data, the Shaw data can be divided according to whether or not cooling rate and anisotropy corrections were applied. Altogether the Shaw paleointensity data represents 6–7% of the whole dataset.

Unfortunately, several publications lack information about the experimental setup as the number of specimens, or samples measured, or the methodology, are not mentioned. Altogether 15% of the Holocene GEOMAGIA50 data do not provide information about the methodology in the publication and are marked as “not specified” in the database.

2.3. Number of samples and specimens measured

The reliability of a given paleointensity data is enhanced if several specimens from the same sample yield the same result, and if several samples from the same locality, each sample representing a cooling unit, yield the same result. For lava flows, Valet (2003) proposes that at least 6 specimens should be measured to get a robust paleointensity determination, but it is difficult to state general rules for different materials. For the last 12,000 years the majority of determinations (68%) rely on single specimen determination (see Fig. 3c).

2.4. Sample size

Sample size is another factor that may influence a paleointensity determination, due to the cooling rate effect (Fox and Aitken, 1980). Aitken et al. (1991) pointed out that the relatively quicker cooling rate for small samples may bias the intensity towards higher values. The majority of data for the last 12,000 years is represented by standard cylinders (40%) and standard cubes (42%) of size similar to 10 cm³. Small (≤ 1 cm³) specimens characterize 10% of the whole dataset. There is only one single-crystal determination.

2.5. Age determination

The reliability of a palaeointensity determination does not depend on the precision and accuracy of the age determination. However, appreciation of dating uncertainties becomes important when the data are compared on a timescale. According to GEOMAGIA50, most of the data (66%) have published age precision between ± 100 years. Data with age precision of ± 500 years represent 22% of the dataset, whereas a minor part has age precision between ± 500 or ± 1000 years (Fig. 3d). We will not discuss here the validity of a certain dating method with respect to others; however we will attempt part of our analysis using only data with age accuracy less than 100 years.

3. Testing paleointensity techniques and materials

In the following we will systematically test the various techniques and materials by, one at the time,

comparing paleointensity data obtained using a certain technique/material with the data obtained using all other techniques/materials. In order to compare data obtained at different geographic locations, the analysis is based on virtual axial dipole moments (VADMs) binned in intervals of 100 and 400 years.

An example is shown in Fig. 4 where paleointensity data obtained from potteries is compared to all remaining data. The figure consists of (a) a scatter plot where the mean VADM for potteries is plotted against the mean VADM for all other data for each 100 year bin (that contains both pottery and other data), (b) two histograms showing the number of data in each of the 100 year bins used for correlation, and (c) a graph of the VADM variation with time for both datasets. To determine the regression line, the solid line in (a), we used the effective variance method (Orear, 1982). This technique is similar to the least square analysis, but accounts for the uncertainties of both variables. In standard least square analysis it is required that one of the variables has no uncertainty, which is not the case here. The uncertainties were estimated first calculating the variance within individual bins and then calculating the weighted variance σ_x^2 and σ_y^2 . The slope b of the regression line was then calculated using the formula:

$$b = \frac{\sigma_x^2 S_y^2 - \sigma_y^2 S_x^2 + \sqrt{(\sigma_y^2 S_x^2)^2 - 2\sigma_x^2 S_y^2 \sigma_y^2 S_x^2 + (\sigma_x^2 S_y^2)^2 + 4S_{xy}^2 \sigma_x^2 \sigma_y^2}}{2S_{xy}^2 \sigma_x^2}$$

where

$$S_x^2 = \frac{\sum_{i=1}^N (x_i - \bar{x})^2}{N - 1}$$

$$S_y^2 = \frac{\sum_{i=1}^N (y_i - \bar{y})^2}{N - 1}$$

$$S_{xy} = \frac{\sum_{i=1}^N (x_i - \bar{x})(y_i - \bar{y})}{N - 1}$$

where \bar{x} and \bar{y} are the mean of the two datasets to be compared, and N is the number of data. The 95% confidence interval for the regression lines (illustrated by connected gray circles) were also calculated using the method described by Paulson (2003). In the case of potteries, the best fitting solid line is close to the ideal 1:1 dashed line (see Fig. 4a), and the correlation coefficient $R=0.76$ is relatively high. This illustrates that paleointensity data from potteries are in good accordance with the remaining dataset, which we interpret to indicate that potteries are a reliable paleointensity recorder. Figs. 5–7 show a similar analysis on methodologies,

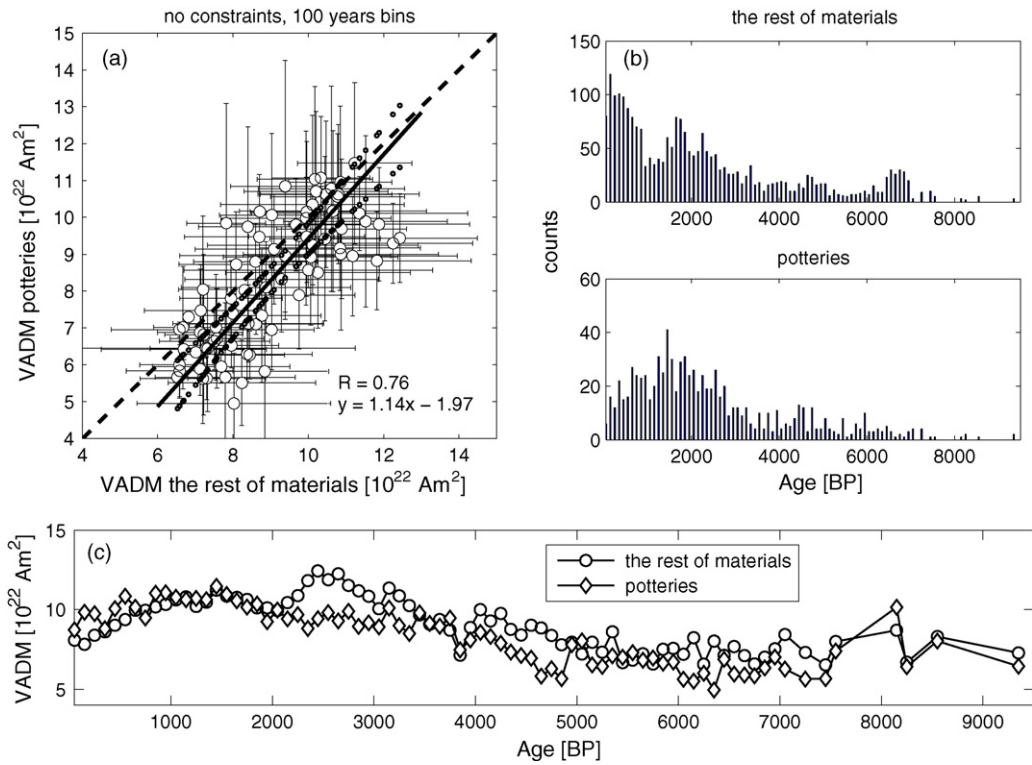


Fig. 4. (a) VADM of potteries plotted against the rest of the dataset, binned in 100 years intervals. Dashed (solid) line represents the 1:1 situation (calculated regression line). Additionally, α_{95} confidence intervals are displayed as connected grey dots. (b) Temporal distribution of the two datasets used for the correlation. “Counts” represents the number of data in each bin. (c) VADM vs. age plot for the two datasets used in the correlation.

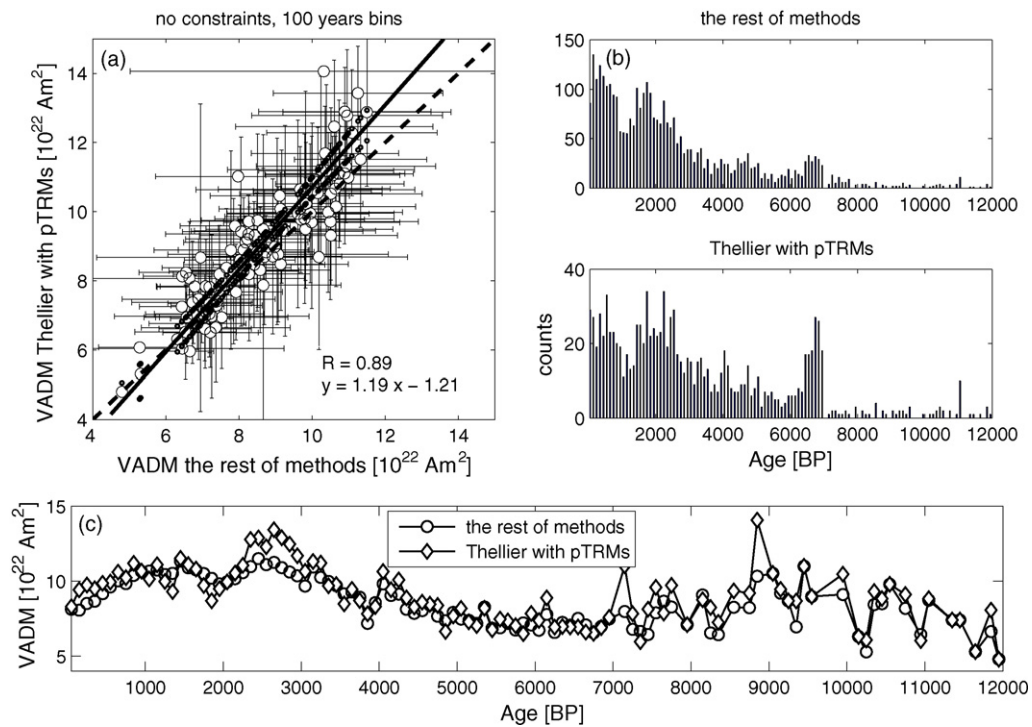


Fig. 5. Correlations for Thellier with pTRM checks vs. the rest of the data. Explanations as in Fig. 4.

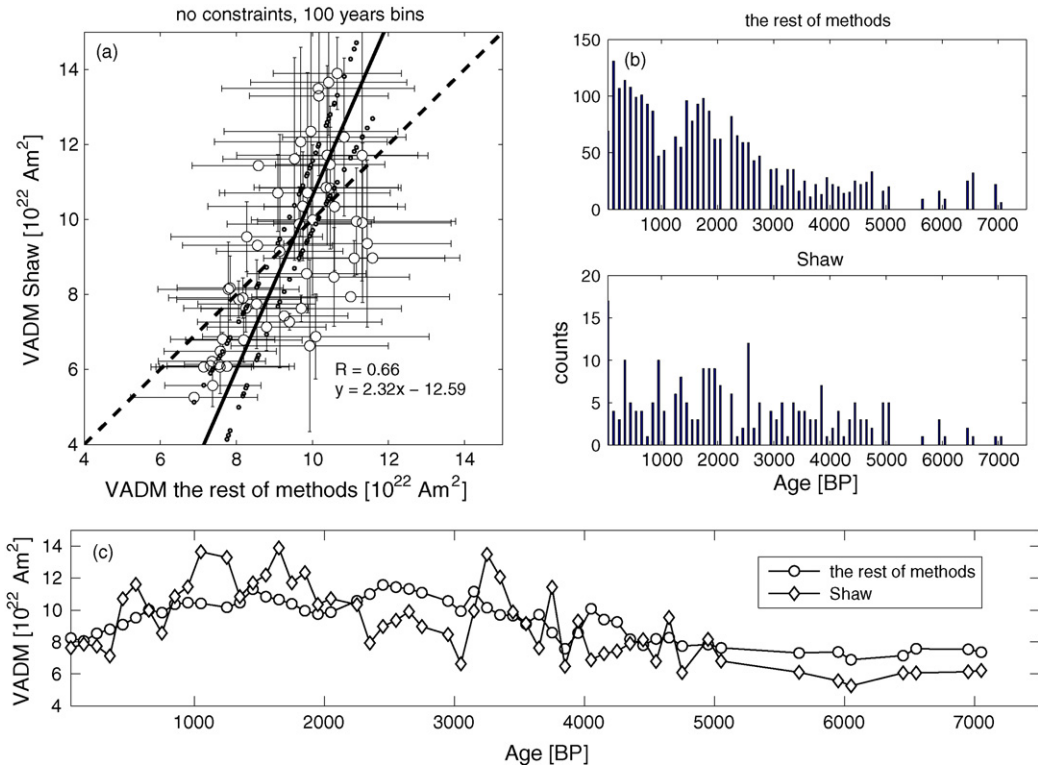


Fig. 6. Correlations for Shaw method vs. the rest of the data. Explanations as in Fig. 4.

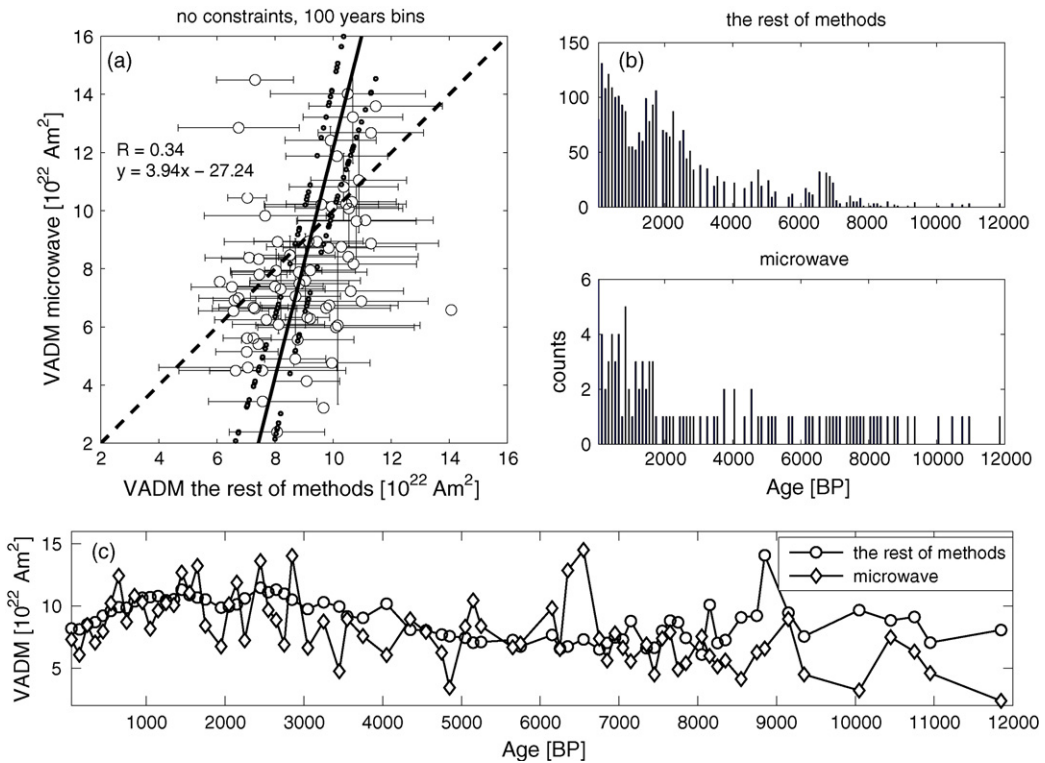


Fig. 7. Correlations for microwave vs. the rest of the data. Explanations as in Fig. 4.

Table 1
VADMs of different materials correlated with all other ones

Material	<i>N</i>	<i>N</i> (%)	<i>N/N</i> _{max} (%)	<i>R</i>	<i>p</i>	Equation
(a and b) 100 years bin						
(a) No constraints (all other materials)						
Ironslags	10	2.0	8.3	0.28	0.42	18.57 <i>x</i> – 182
Kilns	21	4.1	17.5	0.75	9.43E–05	1.88 <i>x</i> – 8.11
Tiles	22	4.3	18.3	0.61	2.00E–03	2.70 <i>x</i> – 16.9
Sun-dried	24	4.7	20.0	0.22	3.00E–01	6.53 <i>x</i> – 52.8
Miscellaneous	42	8.3	35.0	0.46	2.00E–03	3.57 <i>x</i> – 25.54
Bricks	44	8.6	36.7	0.61	0.0001	1.41 <i>x</i> – 3.41
Ovens	50	9.8	41.7	0.52	9.73E–05	1.12 <i>x</i> + 1.11
Ceramics	68	13.4	56.7	0.87	3.13E–22	1.60 <i>x</i> – 5.22
Clays	74	14.5	61.7	0.76	2.67E–15	1.13 <i>x</i> – 1.07
Lava	76	14.9	63.3	0.41	0.0002	1.81 <i>x</i> – 6.53
Potteries	78	15.3	65.0	0.76	5.03E–16	1.14 <i>x</i> – 1.97
(b) Age accuracy constrained to 100 years (all other materials)						
Ironslags	8	2.1	6.7	0.53	1.70E–01	11.78 <i>x</i> + 114
Kilns	21	5.5	17.5	0.77	4.18E–05	1.83 <i>x</i> – 7.53
Tiles	22	5.8	18.3	0.62	0.002	2.36 <i>x</i> – 13.59
Sun-dried	22	5.8	18.3	0.032	0.88	40.45 <i>x</i> – 379
Miscellaneous	41	10.7	34.2	0.46	2.00E–03	3.12 <i>x</i> – 20.73
Bricks	34	8.9	28.3	0.63	5.29E–05	1.90 <i>x</i> – 8.65
Ovens	44	11.5	36.7	0.58	2.77E–05	085 <i>x</i> – 1.18
Ceramics	55	14.4	45.8	0.77	6.38E–12	2.43 <i>x</i> – 13.79
Clays	65	17.0	54.2	0.75	5.98E–13	1.03 <i>x</i> – 0.001
Lava	28	7.3	23.3	0.46	0.014	2.73 <i>x</i> – 16.85
Potteries	42	11.0	35.0	0.39	0.01	0.50 <i>x</i> + 4.72
(c) 400 years bin						
Ironslags	6	3.6	20.0	0.43	0.39	0.10 <i>x</i> + 9.54
Kilns	9	5.4	30.0	0.91	0.0006	0.50 <i>x</i> – 4.95
Tiles	9	5.4	30.0	0.73	0.02	0.56 <i>x</i> – 3.74
Sun-dried	10	6.0	33.3	0.45	0.19	0.47 <i>x</i> + 5.18
Miscellaneous	11	6.6	36.7	0.6	0.05	0.37 <i>x</i> – 6.15
Bricks	15	9.0	50.0	0.7	0.003	0.86 <i>x</i> – 0.60
Ovens	19	11.4	63.3	0.66	0.002	1.31 <i>x</i> – 3.05
Ceramics	19	11.4	63.3	0.95	1.24E–10	0.67 <i>x</i> – 2.82
Clays	21	12.7	70.0	0.91	9.66E–09	1.07 <i>x</i> – 0.85
Lava	24	14.5	80.0	0.51	0.67	0.96 <i>x</i> + 0.89
Potteries	23	13.9	76.7	0.74	5.76E–05	0.96 <i>x</i> – 0.36

(a) The results obtained using no constraints, data binned in 100 years interval. (b) The results obtained using those data with accuracy better than 100 years; data binned in 100 years interval. (c) Correlations obtained without constraints, data binned in 400 years interval. *N* represents the number of bins that are used for calculating the correlation, whereas *N* (%) is the percentage of bins with respect of the sum of all bins used for the correlating the materials. *N/N*_{max} (%) is the percentage of bins used over the maximum possible bin number (i.e. 120 bins for 100 years binning interval over 12,000 years period) for the time period used. *R* is the correlation coefficient and *p* is the probability of random correlation at 95% significant level. The equation of the fitted regression line is also given.

namely Thellier experiments with pTRM checks, Shaw experiments, and microwave experiments. In the case of Thellier experiments with pTRM checks, the best fitting line is close to the ideal 1:1 line (see Fig. 5a), and *R*=0.89 is relatively high. In the two other cases, the regression line is considerably shifted with respect to the ideal 1:1 situation however, this shift may be a result of the small datasets, which do not average well the VADM. We now perform this analysis in a systematic way for each material and method using

two different binning intervals of 100 and 400 years. The results are summarized in terms of number of bins available (*N*), correlation coefficient *R*, correlation probability *p*, and linear regression equation. The results from different materials are represented in Table 1 (a) using 100 years bins and no constraints, (b) selecting only data with dating accuracy better than 100 years, and (c) using 400 years bins. Table 2 shows the results in a similar way for the analyzed methods. In addition, Figs. 8 and 9 show all the best

Table 2
VADMs of different methods correlated with all other ones

Method	N	N (%)	N/N_{\max} (%)	R	p	Equation
(a and b) 100 years bin						
(a) No constraints (all other methods)						
Shaw	54	17.6	45.0	0.66	5.82E-08	$2.32x - 12.59$
Microwave	71	23.2	59.2	0.34	0.003	$3.94x - 27.24$
Thellier	76	24.8	63.3	0.55	2.79E-07	$1.05x - 0.62$
Thellier with pTRM	105	34.3	87.5	0.89	2.60E-37	$1.19x - 1.21$
(b) Age accuracy constrained to 100 years (all other methods)						
Shaw	1	0.7	0.8	–	–	–
Microwave	45	32.6	37.5	0.33	0.02	$4.74x - 40.66$
Thellier	40	29.0	33.3	0.46	0.002	$0.67x + 3.06$
Thellier with pTRM	52	37.7	43.3	0.37	0.005	$0.72x + 4.37$
(c) 400 years bin						
Shaw	18	17.5	60.0	0.78	0.0001	$1.75x - 4.01$
Microwave	30	29.1	100.0	0.39	0.03	$3.19x - 20.66$
Thellier	25	24.3	83.3	0.63	0.0006	$1.06x - 0.77$
Thellier with pTRM	30	29.1	100.0	0.71	1.77E-05	$0.97x + 1.31$

Explanations as for Table 1.

fitting lines for each material and for each method, respectively.

We expect that there are two main factors influencing the observed scatter. One is represented by the experimental error, and the other by the influence of non-dipolar fields during the acquisition of the ancient intensity. Given the inhomogeneous geographical and temporal distribution of the data (Figs. 1 and 2), non-dipole (ND) fields probably influence the analysis. Non-dipole field effects would be better reduced using

virtual dipole moments (VDM) rather than VADM's. However, using VDM's is not feasible since only 863 data (i.e. 25% of the 3425 Holocene data) are directly associated with a paleomagnetic direction. In order to estimate the effect of non-dipole fields, we bin data both in 100 and 400 year intervals. In our analysis we compare the effect of different binning intervals to check the possibility of the influence of non-dipolar fields. The short binning interval (100 years) is advantageous, simply because it produces many binned data-points however,

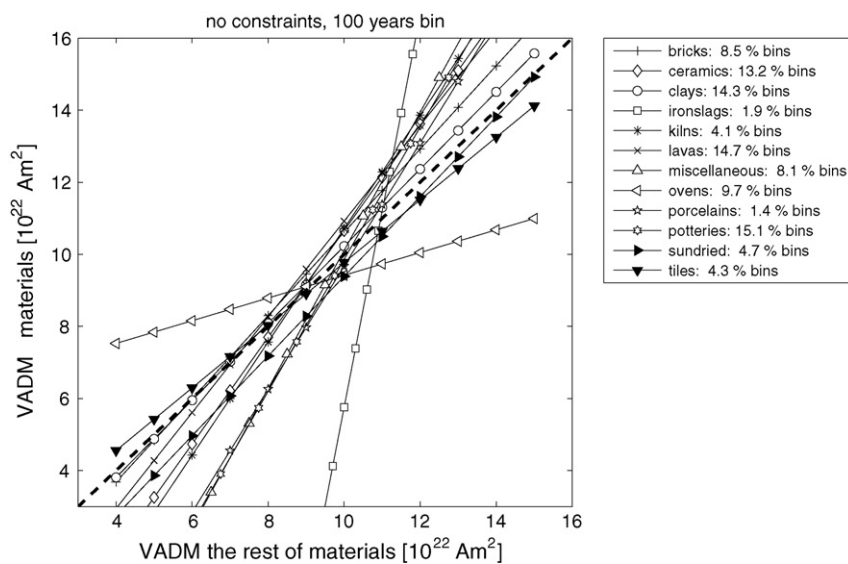


Fig. 8. Scatter plot presenting the regression lines calculated using the effective variance method for all materials included in the GEOMAGIA50 database.

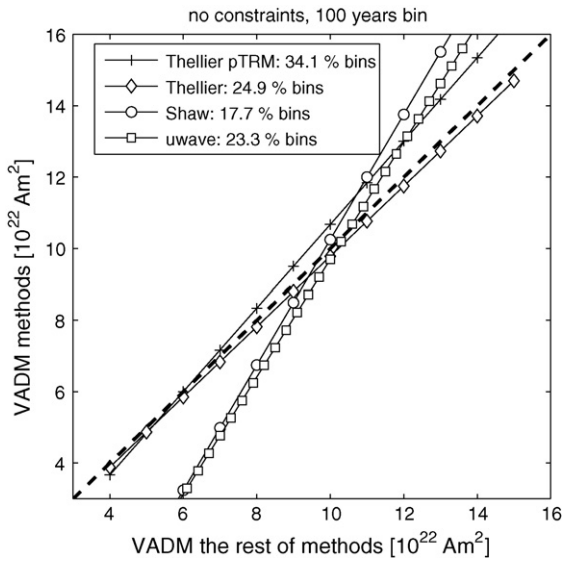


Fig. 9. Scatter plot presenting the regression lines calculated using the effective variance method for the four main techniques included in the GEOMAGIA50 database.

it only poorly averages out secular variation originating from non-dipole-fields. Using the 400 years binning interval, however, shows that the differences are not significant. Some other attempts using a sliding window technique were performed to possibly better average out the ND features. In all cases, we observe that the correlation coefficients and best fitting scatter plot lines are similar irrespective of binning technique and binning-interval-length.

Another way of testing the possible influence of ND features of the geomagnetic field can be performed using the CALS7K.2 model (Korte and Constable, 2005) for the period between 5000 B.C. and 1950 A.D., and the IGRF model for the period between 1950 A.D. and 1998 A.D. This analysis consists of comparing the measured field B_{obs} with the modeled geocentric axial dipole field (B_{gad}), as well as comparing the modeled total field (B_{tot}) with B_{gad} . Theoretically, the difference between the B_{obs} and B_{gad} shows the ND part relating to the direct measurement, whereas the difference between B_{tot} and B_{gad} represents the ND part suggested by the model itself. In practice, the analysis was performed by calculating the field values (both B_{tot} and B_{gad}) for each lava site at the time it acquired the TRM. Fig. 10a and b show histograms representing the observed ND ($B_{\text{obs}} - B_{\text{gad}}$) and the theoretical one ($B_{\text{tot}} - B_{\text{gad}}$). It appears that the differences between observation and model are high. As a comparison we perform the same analysis for the potteries dataset (Fig. 10c and d). Again, it appears that the modeled ND part is significantly lower compared to the

observed one. These observations may partly be due to the CALS7K.2 model smoothing ND contributions both in space and time, but more likely is that the ND field is not responsible for the observed scatter, but that it rather relates to experimental uncertainties. Hence, the variable non-dipole field contribution may play a smaller role compared to the errors introduced by the variable methods and materials.

3.1. Paleointensity materials

The Holocene paleointensity dataset of GEOMAGIA50 distinguishes between 12 different materials plus one group of undefined ones (Fig. 3a). The analysis shows that well-fired archaeological materials (potteries, and clays) best correlate with the rest of the data (Table 1 and Fig. 8), which we interpret to indicate that these materials are good paleointensity recorders. Another feature of the analysis of paleointensity materials is that larger datasets generally correlate better with the rest of the data, whereas smaller datasets show a systematic decrease of R values. This observation reflects that some of the datasets are too small for the analysis, and care should be taken not to focus solely on the correlation coefficient. We do, however, note that for certain materials with fewer data the agreement with the rest of the data is good. For example, bricks and ovens show a regression line close to the ideal 1:1.

Considering the 100 year binning case (Table 1 (a)), ceramics, potteries and clays (68, 78 and 74 bins, respectively) all show high correlation coefficients ($R > 0.75$). Potteries (Fig. 4a) and clays also show an almost 1 to 1 correlation. In contrast, the lava dataset shows more scatter ($R = 0.41$) despite the large number of bins (76) and binned samples. To test whether the slightly larger scatter for lavas is due to dating uncertainties, as lavas in general are more difficult to date than archaeological materials, we also made the analysis for all the materials using only data with age precision better than ± 100 years (see Table 1 (b)). Lavas, like all other datasets show the same trend for age precision better than ± 100 years (Table 1 (b)) as when all data, irrespective of age precision is included (Table 1 (a)). It appears that the observed scatter for lava is not a consequence of inaccurate dating (Table 1 (b)). In general the trend for each material is independent from the age accuracy constrain. Having in mind the ND problem mentioned above, we repeat the analysis using 400 year bins, which better averages out non-dipole fields (Table 1 (c)). Similarly, we observe a low correlation coefficient, which we interpret as a fact that paleointensity data from lavas are noisier compared to archeological artifacts. Although lava

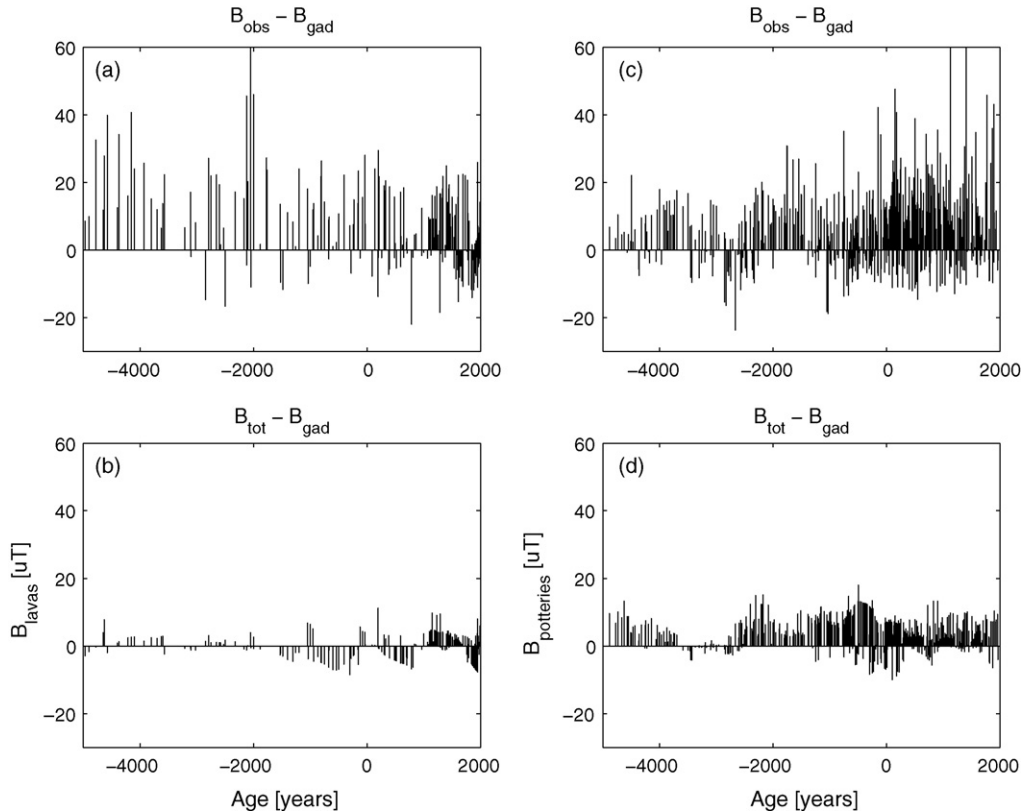


Fig. 10. Simulation of the ND behaviour for lavas (a and b) and potteries (c and d). (a) and (c) present the observed ND contribution, calculated as difference between observed field (B_{obs}) and modeled geocentric axial dipole (B_{gad}). (b) and (d) show the modeled ND contribution, determined as the difference between the modeled total field (B_{tot}) and the modeled B_{gad} .

flows have lower correlation coefficients, we note that the lava regression line is only slightly off the ideal 1:1 line (Fig. 8). This we believe to be a significant observation, which will be discussed further in Section 4.

Fig. 8, which summarizes all the best fit lines calculated, using the effective variance analysis for the 100 year binned data, indicates that most materials correlate well with the rest of the dataset. Only four material types do not follow this trend; namely iron slags, sun-dried archeological objects, miscellaneous objects and tiles. All four data sets are relatively small. In fact, they represent the smallest data sets, all having data in less than 20% of the maximum number of bins. Nevertheless, the offsets are statistically significant, which allows us to question the validity of paleointensity data obtained from these materials. It is perhaps not surprising that iron slags are unsuitable for paleointensity experiments, as they often are so strongly magnetic that their thermoremanent magnetization (TRM) is seriously affected by self-demagnetizing effects. Likewise, it is not surprising that sun-dried objects yield questionable results

as they were heated in the sun only, and therefore never acquired a TRM.

3.2. Paleointensity techniques

We described previously the four main approaches used to determine paleointensity: Thellier with pTRM checks, Thellier without pTRM checks, microwave, and Shaw. These four approaches can be additionally divided by the employment of different strategies used to correct the intensity values; hence GEOMAGIA50 differentiates between 17 different experimental techniques (Fig. 3b). Among these we mention the cooling rate and the anisotropy correction. Despite the importance of cooling rate and anisotropy corrections, they are difficult to quantify and are generally not very large compared to typical experimental errors. Analysis of corrected intensity data versus uncorrected ones is not possible due to the small corrected dataset. We will therefore focus the analysis on the main techniques in order to deal with larger datasets. The analysis of paleointensity techniques is performed

in a similar manner to the analysis of paleointensity materials (Section 3.1). Table 2 shows the correlation coefficients (R) obtained for each method when compared against all other methods. In Table 2 (a) we present the case where paleointensity data were binned in 100 years interval, without constraints. We notice that Thellier with pTRM checks has a good R (0.89), an almost parallel regression line and a similar intercept with the 1:1 situation (Fig. 5a). Thellier without pTRM checks has a fairly high R value (0.55), with a regression line slope close to 1, but it is shifted towards higher values by about half a VADM unit ($1 \times 10^{22} \text{ A m}^2$). In contrast, the situation of the Shaw and microwave methods is more scattered. The scatter plot shows that at lower VADM values the Shaw (Fig. 6) and the microwave (Fig. 7) methodologies produce lower values compared to other techniques, whereas at higher VADM values ($11\text{--}13 \times 10^{22} \text{ A m}^2$) the trend is opposite. Looking at the VADM versus time plot it becomes obvious that the Shaw curve has bigger amplitude variation compared to the rest of the methods. Likewise, the microwave dataset shows a higher variation compared to the rest of the methods. However, this variation might arise from the limited amount of data for the Shaw or the microwave datasets; for example the microwave dataset consists of 5 different studies after Gratton et al. (2005), Casas et al. (2005), Hill and Shaw (1999), Shaw et al. (1996), and Böhnell et al. (2003). In addition, we notice that the majority of microwave data has only 1 study per bin. If we constrain the amount of samples and correlate using data with at least 3 measurements in each bin, then the R improves significantly (0.83), and the curve reduces to the younger period (300–1900 A.D.). However, the variation during this period is still significant. A better agreement is reached when data without lavas are plotted, especially when the two outliers are left out (–800 A.D., after Shaw et al., 1999; and 300 A.D., after Böhnell et al., 2003). In this case, we get a high R (0.88), but the regression line is still off the 1:1 situation.

Table 2 (b) presents the case for data with age accuracy 100 years, binned in 100 year intervals. In this case it appears that the correlation gets significantly lower. In Table 2 (c) we present the correlation results of each dataset binned in 400 year intervals. This case reflects the case of Table 2 (a), showing that the Thellier method has very good correlation parameters. We notice also that Thellier with pTRM checks can improve the correlation if two bins (–10,000 years and –7000 years) which contain one intensity data only are treated as outliers. Fig. 9 presents the plot of the regression lines from the four methodologies calculated using the equation in Table 1 (a).

4. Are lava flows suitable for Thellier paleointensity experiments?

Several authors have pointed out that paleointensity experiments on lava flows are particularly difficult, and, with the potential of producing systematically biased data (Draeger et al., 2006; Gratton et al., 2005; Calvo et al., 2002). A very serious claim was recently put forward that Thellier paleointensity data from lavas are significantly too high, based primarily on experimental tests involving historical lava flows (Yamamoto et al., 2003; Mochizuki et al., 2004; Yamamoto and Tsunakawa, 2005). The proposed reason relates to high-temperature deuteric oxidation, which very often takes place during cooling of lava flows. Using their preferred paleointensity method, which is an extension of the Shaw technique involving low temperature demagnetizations, Yamamoto and Tsunakawa (2005) obtained an average dipole moment of $3.64 \pm 2.10 \times 10^{22} \text{ A m}^2$ for the last 5 million years. This is half the value obtained from all other materials ($7.46 \pm 3.10 \times 10^{22} \text{ A m}^2$), which consist almost exclusively of Thellier results from lavas. They suggest that this difference is caused by Thellier paleointensity estimates being higher than the true values. Since Thellier paleointensity data from high-temperature oxidized lavas constitute a major part of all available pre-Holocene paleointensity data, the suggestion of Yamamoto and Tsunakawa (2005), if true, would significantly affect our understanding of the past geodynamo as well as other geoscience questions that in one way or another relate to the geomagnetic field intensity, as, for example, corrections of cosmogenic radionuclide production for geomagnetic field intensity (Muscheler et al., 2005). Determining the average dipole moment of the past is also crucial to understand the present-day geodynamo and the likelihood of an imminent reversal (Tauxe, 2006). As, discussed above (Section 3.1), lava flow regression lines lie very close to the ideal 1:1 line (Fig. 8), so there are no indications that lava flows may yield results that are significantly offset.

The GEOMAGIA50 database contains 184 Thellier paleointensity estimates from lavas. To test if the Thellier determinations from lava flows yield considerably higher results with respect to other methods, we perform a similar analysis using the Thellier lava dataset and the rest of the data. It should be noticed that a comparison of the dataset of archeological artifacts measured by any Thellier method and the dataset of the archeological artifacts measured by Shaw or microwave technique reveals some discrepancies ($R=0.75$; $y=1.36x-3.69$).

In general we observe that the Thellier lava dataset shows slightly higher values compared to the other data.

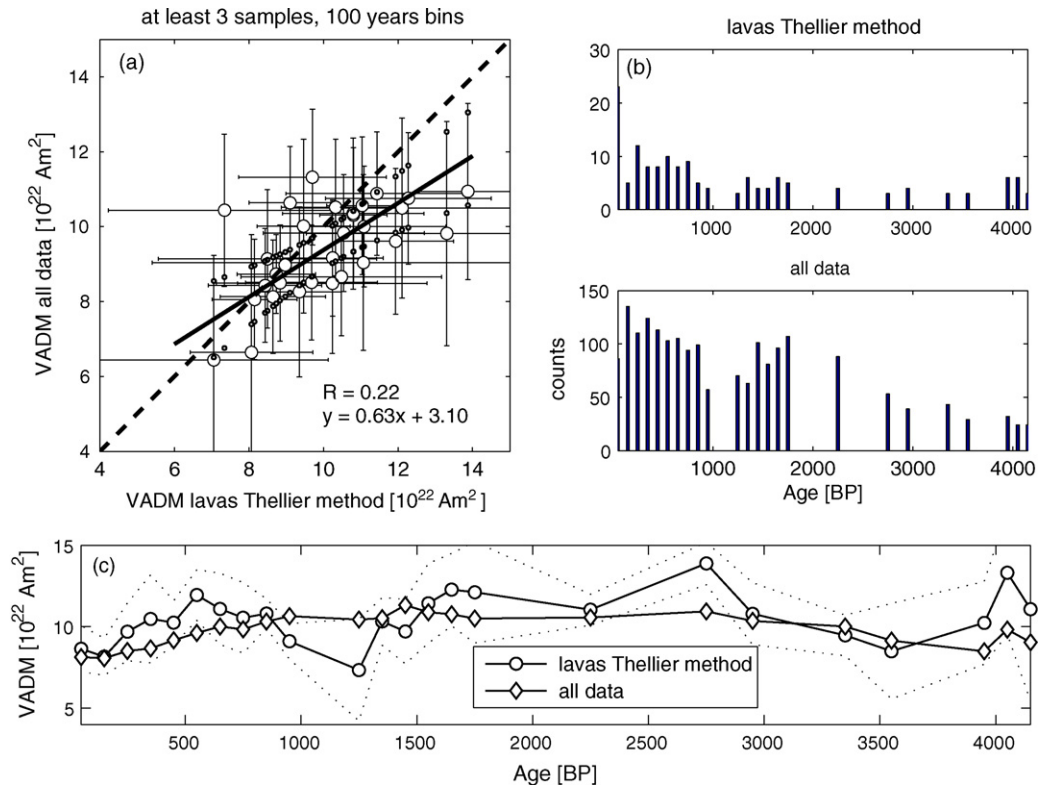


Fig. 11. Comparison of lava data obtained using Thellier vs. all other methods (Shaw and microwaves). Explanations as in Fig. 4.

However, the number of lavas determined by Thellier methods is small, and often there is only one measurement per bin. Therefore, in a further investigation we select only those bins where there are at least three data for each dataset. Using this constraint results in using only the last 4000 years of the curve however we believe this to be a more valid comparison. Our result (Fig. 11) shows a poor degree of correlation ($R=0.22$). The scatter plot shows also that the lavas results are in general shifted toward higher values of VADM. However, the difference appears not to be significant, as the points

of the other materials lie within the standard deviation curve for lavas measured by Thellier methods (Fig. 9c, dotted line). The four points that represent an exception are mentioned in Table 3. Again, the data show that the standard deviations overlaps. In this case a z -test would help decide whether the difference is statistically significant (Table 3). We test the null-hypothesis that there is no true difference between the mean of the lavas and the one of the rest of the dataset for a particular bin. In most cases we can accept the null-hypothesis. Again, the z -test analysis has to be treated with caution because of

Table 3

Binned data for lavas measured with Thellier technique, and binned data measured with any other method

Age	Lavas Thellier method			All other data			
	N	VADM	sVADM	N	VADM	sVADM	z -test
–2100	6	13.3	3.8	18	8.7	1.5	+
–800	3	13.9	1.3	50	10.8	2.3	–
1000	4	9.1	1.1	53	10.8	1.5	+
1400	10	11.9	1.6	93	9.4	1.8	+

Only the data for which the standard deviation envelope for lavas does not include the mean value of “the rest of the data” are presented. The table shows the age for which the discrepancy is observed, the VADM and its standard deviation, and the number of data binned N ; for both lavas and other data. Additionally, the z -test shows if the null hypothesis of no true different means between groups can be accepted (z -test = +) or rejected (z -test = –).

the limited amount of data available for lavas measured by the Thellier method.

5. Conclusions

This is the first study based on the GEOMAGIA50 database. The database is continually updated and freely available on-line at <http://data.geophysics.helsinki.fi>. The quantity of Holocene data is growing rapidly, and future studies can possibly include data-groups that at present are too small for statistically significant analysis, for example paleointensity materials like submarine basaltic glass (e.g. Bowles et al., 2006) and paleointensity methods like microwave. Also, a growing database may allow a better treatment of non-dipole fields, and age-uncertainties. With the limitations of the current database in mind, we restrict ourselves to make only the following general conclusions:

- (i) The only poor correlations we observe are for the materials ironslags, sun-dried archeological objects, miscellaneous objects and tiles. Particular care needs to be taken when using these data. With the exception of these few paleointensity materials, all materials and methods are seen to correlate well with other data. We interpret this to indicate that basically all paleointensity methods and materials yield correct estimates of the ancient field intensity. Some paleointensity methods appear to correlate slightly better than others (Fig. 9 and Table 2) but given the uncertainties related to non-dipole fields and variable number of data, it is not possible to rank the methods.
- (ii) The analysis of lava paleointensity data obtained using the Thellier method does not support the claim of Yamamoto and Tsunakawa (2005) that Thellier experiments on lavas yield significantly too high paleointensities. We observe a slight, but statistically insignificant offset, however, more data are necessary to improve the statistical analysis and show in a clearer way whether the discrepancy is significant or not.

On a final note, we would like to point out that although our analysis is positive in the sense that all Holocene paleointensity methods and materials yield correct results, one cannot draw a general positive conclusion that all paleointensity data are reliable. Extending our Holocene observation into the geological past, one should also consider possible low-temperature alteration that could affect whole-rock lava paleointensity experiments (Smirnov and Tarduno, 2005).

Acknowledgement

We thank Mimi Hill and an anonymous reviewer for their useful comments and discussion which improved this manuscript.

References

- Aitken, M.J., Pesonen, L.J., Leino, M., 1991. The Thellier paleointensity technique: minisamples vs. standard size. *J. Geomag. Geoelectr.* 43, 325–331.
- Bowles, J., Gee, J.S., Kent, D.V., Perfit, M.R., Adam Soule, S., Fornari, D.J., 2006. Paleointensity applications to timing and extent of eruptive activity, 9°–10°N East Pacific Rise. *Geochem. Geophys. Geosyst.* 7, Q06006, doi:10.1029/2005GC001141.
- Böhnel, H., Biggin, A.J., Walton, D., Shaw, J., Share, J.A., 2003. Microwave paleointensities from a recent Mexican lava flow, baked sediments, and reheated potteries. *Earth Planet. Sci. Lett.* 214, 221–236.
- Burlatskaya, S., Nechaeva, T., Petrova, G., 1969. Some archaeomagnetic data indicative of westward drift of the geomagnetic field. *Archeometry* 11, 115–130.
- Calvo, M., Prevot, M., Perrin, M., Riisager, J., 2002. Investigating the reasons for the failure of palaeointensity experiments: a study on historical lava flows from Mt. Etna (Italy). *Geophys. J. Int.* 149, 44–63.
- Casas, L., Shaw, J., Gich, M., Share, J.A., 2005. High-quality microwave archaeointensity determinations from an early 18th century AD English brick kiln. *Geophys. J. Int.* 161, 653–661.
- Chauvin, A., Roperch, P., Levi, S., 2005. Reliability of geomagnetic paleointensity data: the effects of the NRM fraction and concave-up behavior on paleointensity determinations by the Thellier method. *Phys. Earth Planet. Inter.* 150, 265–286.
- Coe, R.S., 1967. Paleointensities of the Earth magnetic field determined from Tertiary and Quaternary rocks. *J. Geophys. Res.* 72, 3247–3262.
- Coe, R.S., Riisager, J., Plenier, G., Leonhardt, R., Krasa, D., 2004. Multidomain behavior during Thellier paleointensity experiments: results from the 1915 Mt. Lassen flow. *Phys. Earth Planet. Inter.* 147, 141–153.
- Collinson, D.W., 1993. Magnetism of the Moon—a lunar core dynamo of impact magnetization. *Surv. Geophys.* 14, 89–118.
- Constable, C., Korte, M., 2006. Is Earth's magnetic field reversing? *Earth Planet. Sci. Lett.* 246 (1–2), 1–16.
- Cottrell, R.D., Tarduno, J.A., 1999. Geomagnetic paleointensity derived from single plagioclase crystals. *Earth Planet. Sci. Lett.* 169, 1–5.
- Donadini, F., Korhonen, K., Riisager, P., Pesonen, L.J., 2006. Database for Holocene geomagnetic intensity information. *EOS Trans. Am. Geophys. Union* 87 (14), 137.
- Draeger, U., Prévot, M., Poidras, T., Riisager, J., 2006. Single-domain chemical, thermochemical and thermal remanences in a basaltic rock. *Geophys. J. Int.* 166, 12–32.
- Fox, J.M.W., Aitken, M.W., 1980. Cooling-rate dependence of thermomagnetic magnetization. *Nature* 283, 462–463.
- Gallet, Y., Genevey, A., Fluteau, F., 2005. Does Earth's magnetic field secular variation control centennial climate change? *Earth Planet. Sci. Lett.* 236, 339–347.

- Genevey, A., Gallet, Y., 2002. Intensity of the geomagnetic field in western Europe over the past 2000 years: New data from ancient French pottery. *J. Geophys. Res.* 107, 1–18.
- Glatzmaier, G.A., Coe, R.S., Hongre, L., Roberts, P.H., 1999. The role of the Earth's mantle in controlling the frequency of geomagnetic reversals. *Nature* 401, 885–890.
- Gómez-Paccard, M., Chauvin, A., Lanos, Ph., Thiriot, J., Jiménez-Castillo, P., 2006. Archeomagnetic study of seven contemporaneous kilns from Murcia (Spain). *Phys. Earth Planet. Interiors* 157, 16–32.
- Gratton, M.N., Shaw, J., Herrero-Bervera, E., 2005. An absolute paleointensity record from SOH1 lava core, Hawaii, using microwave technique. *Phys. Earth Planet. Inter.* 148, 193–214.
- Halls, H.C., McArdle, N.J., Gratton, M.N., Hill, M.J., Shaw, J., 2004. Microwave paleointensities from dyke chilled margins: a way to obtain long-term variations in geodynamo intensity for the last three billion years. *Phys. Earth Planet. Inter.* 147, 183–195.
- Heller, R., Merrill, R.T., McFadden, P.L., 2002. The variation of intensity of earth's magnetic field with time. *Phys. Earth Planet. Inter.* 131, 237–249.
- Hill, M.J., Gratton, M.N., Shaw, J., 2002. A comparison of thermal and microwave palaeomagnetic techniques using lava containing laboratory induced remanence. *Geophys. J. Int.* 151, 157–163.
- Hill, M.J., Shaw, J., 2000. Magnetic field intensity study of the 1960 Kilauea lava flow, Hawaii, using the microwave palaeointensity technique. *Geophys. J. Int.* 142, 487–504.
- Hill, M., Shaw, J., 1999. Paleointensity results for historic lavas from My. Etna using microwave demagnetization/remagnetization in a modified Thellier-type experiment. *Geophys. J. Int.* 139, 583–590.
- Hulot, G., Eymin, C., Langlais, B., Manda, M., Olsen, N., 2002. Small-scale structure of the geodynamo inferred from the Oersted and Magsat satellite data. *Nature* 416, 620–623.
- Jackson, A., Jonkers, A.R.T., Walker, M.R., 2000. Four centuries of geomagnetic secular variation from historical records. *Phil. Trans. R. Soc. Lond.* 358, 957–990.
- Korhonen, K., Donadini, F., Riisager, P., Pesonen, L.J. Implementation of the GEOMAGIA50 database application, in preparation.
- Korte, M., Constable, C.G., 2005. The geomagnetic dipole moment over the last 7000 years—new results from a global model. *Earth Planet. Sci. Lett.* 236, 348–358.
- Krasa, D., Heunemann, C., Leonhardt, R., Petersen, N., 2003. Experimental procedure to detect multidomain remanence during Thellier–Thellier experiments. *Phys. Chem. Earth* 28, 681–687.
- Mochizuki, N., Tsunakawa, H., Oishi, Y., Wakai, S., Wakabayashi, K.I., Yamamoto, Y., 2004. Palaeointensity study of the Oshima 1986 lava in Japan: implications for the reliability of the Thellier and LTD-DHT Shaw methods. *Phys. Earth Planet. Inter.* 146, 395–416.
- Muscheler, R., Joos, F., Muller, S.A., Snowball, I., 2005. Climate—How unusual is today's solar activity? *Nature* 436, E3–E4.
- Oishi, Y., Tsunakawa, H., Mochizuki, N., Yamamoto, Y., Wakabayashi, K.I., Shibuya, H., 2005. Validity of the LTD-DHT Shaw and Thellier palaeointensity methods: a case study of the Kilauea 1970 lava. *Phys. Earth Planet. Inter.* 149, 243–257.
- Olsen, N., 2002. A model of the geomagnetic field and its secular variation for epoch 2000 estimated from Oersted data. *Geophys. J. Int.* 149, 454–462.
- Orear, J., 1982. Least squares when both variables have uncertainties. *Am. J. Phys.* 50 (10), 912–916.
- Pan, Y.X., Shaw, J., Zhu, R.X., Hill, M.J., 2002. Experimental reassessment of the Shaw paleointensity method using laboratory-induced thermal remanent magnetization. *J. Geophys. Res.* 107 (B7) (Art. No. 2129).
- Paulson, D.J., 2003. *Applied Statistical Design for the Researcher*. Marcel Dekker Publisher, New York, ISBN 0824740858, 712 pp.
- Pesonen, L.J., Leino, M.A.H., Nevanlinna, H., 1995. Archeomagnetic intensity in Finland during the last 6400 years: Evidence for a latitude-dependent nondipole field and ~AD 500. *J. Geomag. Geoelectr.* 47, 19–40.
- Pick, T., Tauxe, L., 1993. Holocene paleointensities—Thellier experiments of submarine basaltic glass for the East Pacific Rise. *J. Geophys. Res.* 98 (B10), 17949–17964.
- Riisager, P., Riisager, J., 2001. Detecting multidomain grains in Thellier palaeointensity experiments. *Phys. Earth Planet. Inter.*, 125.
- Riisager, P., Riisager, J., Abrahamson, N., Waagstein, R., 2002. Thellier palaeointensity experiments on Faroes flood basalts: technical aspects and geomagnetic implications. *Phys. Earth Planet. Inter.* 131, 91–100.
- Selkin, P.A., Tauxe, L., 2000. Long-term variations in palaeointensity. *Phil. Trans. R. Soc. Lond. Series A* 358, 1065–1088.
- Shaw, J., 1974. A new method of determining the magnitude of the palaeomagnetic field; application to five historic lavas and five archaeological samples. *Geophys. J. R. Astronom. Soc.* 39, 133–141.
- Shaw, J., Walton, D., Yang, S., Rolph, T.C., Share, J.A., 1996. Microwave paleointensities from Peruvian ceramics. *Geophys. J. Int.* 124, 241–244.
- Shaw, J., Yang, S., Rolph, T.C., Sun, F.Y., 1999. A comparison of archaeointensity results from Chinese ceramics using microwave and conventional Thellier's and Shaw's methods. *Geophys. J. Int.* 136, 714–718.
- Shaw, J., Hill, M.J., Openshaw, S.J., 2001. Investigating the ancient Martian magnetic field using microwaves. *Earth Planet. Sci. Lett.* 190, 103–109.
- Shcherbakova, V.V., Shcherbakov, V.P., 2000. Properties of partial thermoremanent magnetization in pseudosingle domain and multidomain grains. *J. Geophys. Res.* 105, 767–781.
- Smirnov, A.V., Tarduno, J.A., 2005. Thermochemical remanent magnetization in Precambrian rocks: Are we sure the geomagnetic field was weak? *J. Geophys. Res.* 110 (Art. No. B06103).
- Stevenson, D.J., 2001. Mars' core and magnetism. *Nature* 412, 214–219.
- Tarduno, J.A., Cottrell, R.D., 2005. Dipole strength and variation of the time-averaged reversing and nonreversing geodynamo based on Thellier analyses of single plagioclase crystals. *J. Geophys. Res.* 110 (Art. No. B11101).
- Tarduno, J.A., Cottrell, R.D., Smirnov, A.V., 2006. The paleomagnetism of single silicate crystals: recording geomagnetic field strength during mixed polarity intervals, superchrons, and inner core growth. *Rev. Geophys.* 44 (Art. No. RG1002).
- Tarling, D.H., Hammo, N.B., Downey, W.S., 1986. The scatter of magnetic directions in archaeomagnetic studies. *Geophysics* 51 (3), 634–639.
- Tauxe, L., 2006. Long-term trends in paleointensity: the contribution of DSDP/ODP submarine basaltic glass collections. *Phys. Earth Planet. Inter.* 156, 223–241.
- Thellier, E., Thellier, O., 1959. Sur l'intensité du champ magnétique terrestre dans le passé historique et géologique. *Ann. Geophys.* 15, 285–376.
- Valet, J.P., 2003. Time Variations in geomagnetic intensity. *Rev. Geophys.* 41, 1004, doi:10.1029/2001RG000104.
- Veitch, R.J., Hedley, I.G., Wagner, J.J., 1984. An investigation of the intensity of the geomagnetic field during Roman times using

- magnetically anisotropic bricks and tiles. *Archives des Sciences Genève* 37, 359–373.
- Walton, D., 1991. A new technique for determining palaeomagnetic intensities. *J. Geomagnet. Geoelectric.* 43, 333–339.
- Weiss, B.P., Vali, H., Baudenbacher, F.J., Kirschvink, J.L., Stewart, S.T., Shuster, D.L., 2002. Records of an ancient Martian magnetic field in ALH84001. *Earth Planet. Sci. Lett.* 201, 449–463.
- Yamamoto, Y., Tsunakawa, H., 2005. Geomagnetic field intensity during the last 5 Myr: LTD-DHT Shaw palaeointensities from volcanic rocks of the Society Islands, French Polynesia. *Geophys. J. Int.* 162, 79–114.
- Yamamoto, Y., Tsunakawa, H., Shibuya, H., 2003. Palaeointensity study of the Hawaiian 1960 lava: implications for possible causes of erroneously high intensities. *Geophys. J. Int.* 153, 263–276.
- Yu, Y.J., Tauxe, L., Genevey, A., 2004. Toward an optimal geomagnetic field intensity determination technique. *Geophys. Geochem. Geosyst.* 5 (Art. No. Q02H07).